



Defect-mediated ferroelectric domain depinning of polycrystalline BiFeO₃ multiferroic thin films

I. Bretos, R. Jiménez, C. Gutiérrez-Lázaro, I. Montero, and M. L. Calzada

Citation: *Applied Physics Letters* **104**, 092905 (2014); doi: 10.1063/1.4867703

View online: <http://dx.doi.org/10.1063/1.4867703>

View Table of Contents: <http://scitation.aip.org/content/aip/journal/apl/104/9?ver=pdfcov>

Published by the *AIP Publishing*

Articles you may be interested in

The effects of La substitution on ferroelectric domain structure and multiferroic properties of epitaxially grown BiFeO₃ thin films

Appl. Phys. Lett. **103**, 132907 (2013); 10.1063/1.4822327

Structural, dielectric, ferroelectric and piezoresponse force microscopy characterizations of bilayered Bi_{0.9}Dy_{0.1}FeO₃/K_{0.5}Na_{0.5}NbO₃ lead-free multiferroic films

J. Appl. Phys. **112**, 052008 (2012); 10.1063/1.4746086

Strain effect on the surface potential and nanoscale switching characteristics of multiferroic BiFeO₃ thin films

Appl. Phys. Lett. **100**, 132907 (2012); 10.1063/1.3698155


Polarization fatigue of Pr and Mn co-substituted BiFeO₃ thin films

Appl. Phys. Lett. **99**, 012903 (2011); 10.1063/1.3609246

Structural changes and ferroelectric properties of BiFeO₃ – PbTiO₃ thin films grown via a chemical multilayer deposition method


J. Appl. Phys. **105**, 014101 (2009); 10.1063/1.3053773

Agilent's Electronic Measurement Group is becoming **Keysight Technologies**.



Engineering Education & Research Resources DVD 2014

Agilent is the key to your test and measurement needs **Order yours**



Defect-mediated ferroelectric domain depinning of polycrystalline BiFeO₃ multiferroic thin films

I. Bretos,^{a)} R. Jiménez, C. Gutiérrez-Lázaro, I. Montero, and M. L. Calzada

Instituto de Ciencia de Materiales de Madrid (ICMM), Consejo Superior de Investigaciones Científicas (CSIC), Sor Juana Inés de la Cruz 3, 28049, Madrid, Spain

(Received 8 November 2013; accepted 20 February 2014; published online 5 March 2014)

The ferroelectric domain depinning in a polycrystalline BiFeO₃ film is studied by a defect-mediated diffusion mechanism driven by a secondary re-oxidation anneal. The presence of defect complexes (oxygen-vacancy-associated dipoles) responsible for pinning is discussed from the current-voltage (I-V) characteristics of the film. Dissociation of these complexes by re-oxidation anneal produces the effective depinning of domains in the material. The released oxygen vacancies would be compensated at the re-oxidized state due to the valence change of Fe²⁺ to Fe³⁺. Improvement on domain mobility results in a larger contribution to ferroelectric switching, showing a room-temperature remanent polarization of 67 μC cm⁻². © 2014 AIP Publishing LLC. [<http://dx.doi.org/10.1063/1.4867703>]

The bismuth ferrite (BiFeO₃) perovskite remains considered the most competitive compound among single-phase multiferroics nowadays.¹ One of the reasons lies on its high Curie (1103 K) and Néel (643 K) temperatures, which allow displaying both ferroelectricity and G-type antiferromagnetism at room temperature. Today, the development of potential BiFeO₃ devices is however focused on its ferroelectric character. With the highest polarization among perovskite oxides predicted ($P_r \sim 100 \mu\text{C cm}^{-2}$),² it took several decades until this could be experimentally measured in thin films only few years ago,³ confirming its intrinsic nature soon afterward in single crystals.⁴ The main obstacle is associated with the high electrical conductivity of the material that prevents an optimum ferroelectric polarization at room temperature.⁵ In this context, the presence of impurities (nonstoichiometry, secondary phases) and charged defects are considered crucial with regard the large leakage currents observed in BiFeO₃,⁶ which has limited its application for a long time. Recently, the existence of non-neutral (head-to-head) domain walls that are electrically compensated by trapping of mobile charges has been observed in the 180° polarization switching of BiFeO₃ epitaxial films.⁷ The stabilization of this configuration produces a strong domain-wall pinning in the material responsible for the intrinsic polarization fatigue (and suppression⁸) observed. Improvement on domain dynamics, e.g., by releasing a domain-wall pinned structure, may significantly enhance the ferroelectric polarization of the film allowing higher saturation values that would make the material suitable for practical applications.⁹ In this Letter, we demonstrate the effective depinning of BiFeO₃ thin films by means of a defect-mediated diffusion mechanism that results in a domain configuration with increased mobility and large ferroelectric response.

Polycrystalline BiFeO₃ multiferroic thin films (240 nm) were grown on Pt/TiO₂/SiO₂/(100)Si substrates by a solution method reported elsewhere.¹⁰ Ten layers of this solution were successively deposited and pyrolyzed before the whole stack was crystallized by rapid thermal annealing (RTA) at

773 K for 60 s in air. The resulting as-crystallized sample will be denoted as “fresh” BiFeO₃ film. For the purpose of this study, a subsequent thermal treatment in static oxygen was applied to this sample in a furnace at 573 K for 30 min (10 K min⁻¹). The resulting postannealed sample will be denoted as “re-oxidized” BiFeO₃ film. X-ray diffraction (XRD) and scanning electron microscopy (SEM) examinations revealed no change in the structure and surface morphology upon reoxidation annealing. A planar array of discrete capacitors was formed in the BiFeO₃ films by sputtering Pt/Au top electrodes on their surface through a shadow mask. Ferroelectric characterization of the samples was carried out using a Radiant Precision Premier II materials analyzer, a HP-8116A pulse generator, a Keithley-K428 current amplifier, and a Tektronix-TDS520 oscilloscope. Impedance spectroscopy was carried out with a HP-4284A LCR Meter (signal 0.01 V) and a lock-in amplifier DSP7265 for low-frequency measurements. X-ray photoelectron spectroscopy (XPS) was performed in a VGS ESCALAB 210 instrument using a nonmonochromatic Mg K α x-ray source ($h\nu = 1253.6 \text{ eV}$) at normal emission angle and 20 eV pass energy.

Figure 1 shows the ferroelectric hysteresis loops measured on the *fresh* BiFeO₃ film at different temperatures. Contrary to the common issue of conducting BiFeO₃,⁵ the sample of this work presents a relatively high resistivity at zero DC bias ($>10^{11} \Omega \text{ cm}$). Room-temperature polarization [Fig. 1(a)] at low voltages (sub-switching fields) results in a slim loop with no ferroelectric contribution. However, upon voltage increase, domain switching starts to occur together with a significant non-linear conduction that suppresses ferroelectric polarization of the film by reaching an irreversible dielectric breakdown at 7 V (not shown). This behavior was unfortunately repeated in a number of capacitors and reproduced for several samples of *fresh* BiFeO₃ films. To gain insight into the polarization process, we minimized the leakage current contribution in this film by low-temperature measurements at 200 K [Fig. 1(b)]. The resulting hysteresis curve reveals now a pinched-like shape very similar to that found in recent reports on pinned BiFeO₃ bulk ceramics.^{11,12}

^{a)} Author to whom correspondence should be addressed. Electronic mail: ibretos@icmm.csic.es

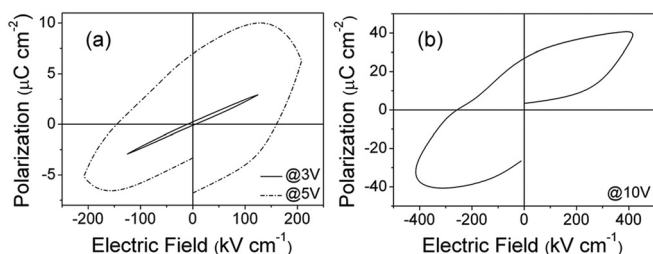


FIG. 1. Polarization hysteresis P vs E of the *fresh* BiFeO₃ film measured at room temperature (a) and 200 K (b) at a frequency of 1 kHz.

Constriction of ferroelectric loops (“pinching”) is generally indicative of domain pinning in the material, usually induced by point defects and/or oxygen-vacancy-combined defect dipoles. Despite the reduced conductivity and the higher voltage applied in the film at this temperature, complete switching of ferroelectric domains is still not observed for positive voltages, what suggests the “hardening” of the sample due to the presence of aligned oxygen-vacancies-associated dipoles.¹³ The polycrystalline nature of this film, with grains revealed as being in a monodomain state,¹⁰ may lead to the formation of non-neutral grain boundaries in the material that would be electrically compensated by the former defect species, thus pinning the associated domain in an analogous situation to that shown for BiFeO₃ epitaxial films with electrically uncompensated domain walls.⁷ From this first analysis, we can state that the initial configuration of the *fresh* BiFeO₃ film is close to a hard ferroelectric material with ferroelectric domains strongly pinned by local defects.

The current-voltage (I - V) curves at room temperature for the *fresh* BiFeO₃ film are shown in Figure 2. Successive measurements were carried out at maximum voltages of 3 V, 5 V, and 3 V back, depicted from Figs. 2(a) to 2(c), respectively. At low voltages [Fig. 2(a)], the film exhibits a high resistance state (HRS) which relates to the low dielectric loss of the capacitor at zero voltage (0.044). The stabilization of a domain configuration strongly pinned by defects may

explain the reduced leakage current observed at this voltage. Oxygen vacancies present in the film can be located at the pinning centers (as defect dipoles) not contributing to any mechanism increasing the concentration of electronic charge carriers. However, when the maximum voltage is increased up to 5 V [Fig. 2(b)], the film changes its state to a low resistance one (LRS) that would account for the increased conduction measured in the corresponding ferroelectric loop of Fig. 1(a). The application of switching voltages in this film produces a strong charge motion out of traps which severely degrades the electrical performance of the material. Oxygen vacancies resealed from the pinning centers would act as donors in the system leading to the high leakage current measured. It is worth noting that the sample holds irreversibly on this conductive state despite decreasing the voltage again down to 3 V [Fig. 2(c)], what rules out any resistance switching behavior on this film.¹⁴

We have studied the effect of a postannealing in oxygen on the leakage characteristics of the resulting *re-oxidized* BiFeO₃ film, whose corresponding I - V curves appear included in Figure 2. The concentration of oxygen vacancies, which play an important role in the electric transport properties of ferroelectric perovskites, is known to decrease after conditioning treatments in oxidative atmospheres.¹⁵ Interestingly, the dielectric loss of the film at zero voltage becomes now larger (0.060) and higher levels of leakage current (almost three orders of magnitude) are measured at 3 V [Fig. 2(a)] with respect to the *fresh* sample. This behavior is indicative of a greater amount of free $V_{O}^{\bullet\bullet}$ in the system after treatment that contributes to the increased electronic conduction of the film. However, the concentration of these species is lower with respect to that arisen in the *fresh* film after electrical degradation, i.e., when dissociation of defect dipoles is produced by the high electric fields responsible for the low resistance state of the sample. Thus, when voltages close to ferroelectric switching are applied [Fig. 2(b)], the *re-oxidized* BiFeO₃ film shows a symmetric and mostly reversible curve in contrast to the *fresh* one. Note that degradation of

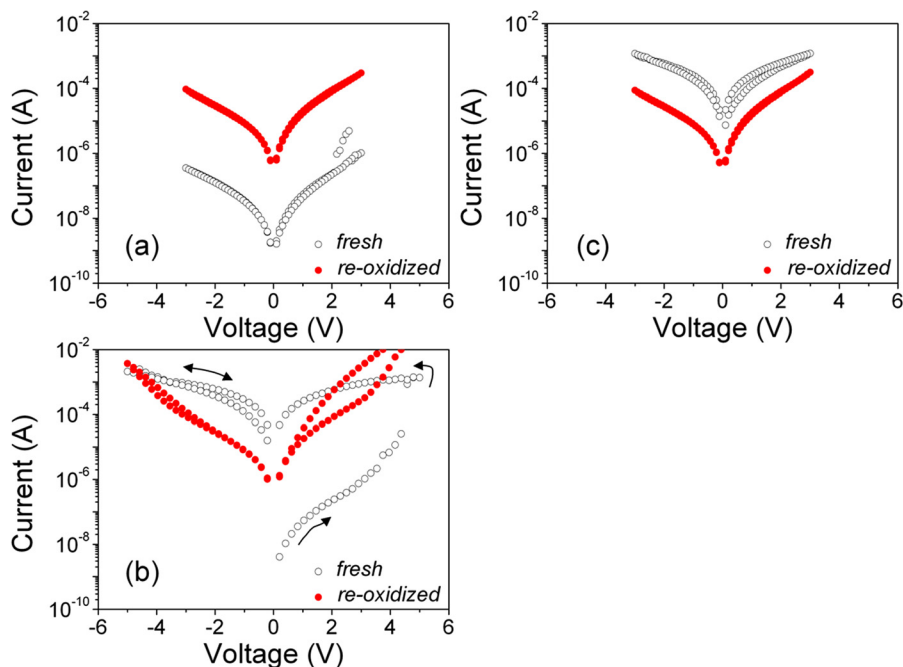
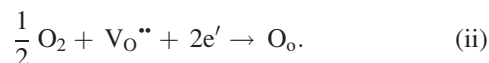
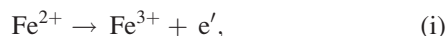


FIG. 2. Current-voltage I vs V curves of the *fresh* and *re-oxidized* BiFeO₃ film measured at room temperature with successive 3 (a), 5 (b), and 3 V back (c) maximum voltages.

the capacitor after this voltage level is not observed in the former film with values of leakage current comparatively lower at 3 V back [Fig. 2(c)]. The *re-oxidized* BiFeO₃ film showed a dielectric loss at zero voltage of 0.026 after this series of electrical measurements, whereby the local defects were expected to diffuse generating a new domain structure in the material. Therefore, the results obtained from this figure point to an improved domain mobility in the BiFeO₃ films of this work after the re-oxidation anneal. The effect of this process on the defect equilibrium of the films is described as follows:

- (1) A ferroelectric domain configuration strongly pinned by local defects is assumed for the *fresh* BiFeO₃ film. The use of a bismuth excess in the precursor solution¹⁰ would compensate for the V_{Bi}''' generated by volatilization from the film, leaving the V_{O}'' defect as the main candidate responsible for pinning.
- (2) Postannealing in oxygen, however, results in higher dielectric losses at zero DC bias. The mechanism causing this response may be associated with the presence of pair centers in the *fresh* BiFeO₃ film resulting from the combination of oxygen vacancies with transition metal ions.¹⁶ In agreement with other authors,¹² we propose the plausible formation of the $\text{Fe}^{2+}-V_{\text{O}}''$ defect dipole during crystallization that would incorporate (freeze) into electrostatically non-neutral grain boundaries of the film, acting thus as pinning center. The V_{O}'' species forming the pinning dipoles would not contribute to any conduction mechanism involving the generation of charge carriers in the film.
- (3) Dissociation of this defect complex with the re-oxidation anneal (via thermal energy) produces depinning of ferroelectric domains in the film. The released species (Fe^{2+} and V_{O}'') may interact with the surrounding O₂ atmosphere resulting in iron oxidation (i) and compensation for oxygen vacancies (ii) according to the complementary reactions



The presence of mobile, free V_{O}'' species out of the pinning centers contributes to the generation of conducting electrons that would be responsible for the relatively high leakage currents measured (Fig. 2(a)).

The defect-mediated mechanism leading to ferroelectric domain depinning in the film is supported by Figure 3. The fitting analysis of the XPS spectra shown in Fig. 3(a) denotes the coexistence of both Fe^{3+} (711.4 eV) and Fe^{2+} (709.1 eV) states in the BiFeO₃ samples due to the common valence fluctuation of this ion.¹⁷ However, the $\text{Fe}^{3+}/\text{Fe}^{2+}$ ratio calculated from the integration of the corresponding fitting curves at the Fe 2p_{3/2} level (including satellites peaks) is 0.809 and 1.041 for the *fresh* and *re-oxidized* film, respectively. This means a relative increase in the Fe^{3+} concentration of 6.3% after dissociation of the $\text{Fe}^{2+}-V_{\text{O}}''$ complex following reaction (i). The release of electrons to the system contributes to the raise of the electrical conductivity of the BiFeO₃ film, as clearly shown by Fig. 3(b). The DC resistivity calculated from the plateau of the real part of admittance with frequency results two order of magnitude lower in the *re-oxidized* film ($6.7 \times 10^{10} \Omega \text{ cm}$) with respect to the *fresh* one ($2.5 \times 10^{12} \Omega \text{ cm}$), which accounts for the higher dielectric loss and leakage current observed at moderate voltages after ferroelectric domain depinning. To corroborate the effectiveness of this process, Figure 4 shows the ferroelectric properties of the *re-oxidized* BiFeO₃ film by hysteresis [Fig. 4(a)] and pulsed polarization [Fig. 4(b)] measurements at room temperature. Experimental loop (open circles) of ferroelectric hysteresis is plotted as the variation of charge current with the electric field. An optimum switching of ferroelectric domains is deduced for this film from the symmetric dual peaks observed at an average coercive field of $\sim 400 \text{ kV cm}^{-1}$. Non-switching contributions arisen from linear capacitance and resistance effects, as well as from non-linear conduction (leakage current), were subtracted from the experimental loop of Fig. 4(a) by a simulation model¹⁸ using a fitting algorithm based on an implemented hyperbolic tangent function.¹⁹ Note the high accuracy between the experimental and simulated data (solid line), from which the compensated charge current loop (closed circles) is obtained. The integration of this loop results in the plot of polarization versus electric field, which appears in the inset of this figure. A remanent polarization of $67 \mu\text{C cm}^{-2}$ (P_r) is obtained for the *re-oxidized* film, being among the highest values reported to date for thin films of this multiferroic composition.^{3,7,8,20} This result is confirmed by the pulsed polarization characteristics shown in Fig. 4(b). The integration of the switching current transitory between two consecutive reading pulses in the poled sample yields a pulsed, non-volatile polarization of $110 \mu\text{C cm}^{-2}$ ($2P_r$). Improvement on ferroelectric switching by a defect-mediated mechanism for domain depinning is

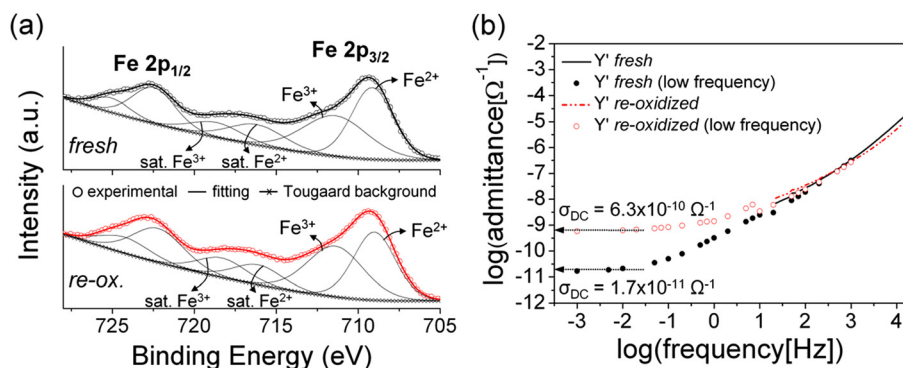


FIG. 3. (a) Fe 2p core levels XPS spectra showing in brackets peak maximum and FWHM width (eV) of fitting curves (sat. = satellite) and (b) variation of the real part of admittance (Y') with frequency in the *fresh* and *re-oxidized* BiFeO₃ film measured with a LCR meter (lines) and a lock-in amplifier (symbols) for low-frequency measurements.

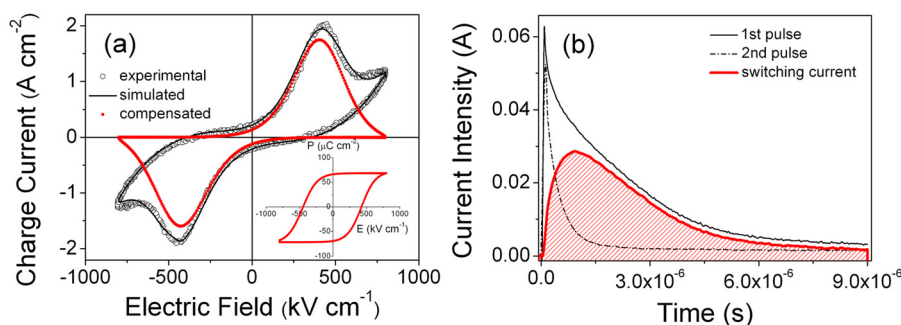


FIG. 4. (a) Charge current hysteresis J vs E of the *re-oxidized* BiFeO₃ film measured at room temperature and 5 kHz frequency. Experimental (open circles), simulated (solid line), and compensated (closed circles) curves are depicted. The equivalent P vs E graph resulting from the integration of the compensated J vs E loop appears in the inset. (b) Switching current transitory measured at room temperature between two consecutive reading pulses (14 V amplitude, 2 μ s width) separated by 10 μ s after the application of a train of pulses with opposite sign (2 μ s width) at the writing voltage in a poled *re-oxidized* BiFeO₃ film. Integration of the difference area (filled under curve) gives rise to the pulsed non-volatile polarization.

thus revealed as a powerful strategy to achieve large polarization values at room temperature in BiFeO₃ thin films.

In summary, ferroelectric domain depinning in a polycrystalline BiFeO₃ thin film is studied by a defect-mediated diffusion mechanism driven by a secondary re-oxidation anneal. Comparison of I-V curves between the *fresh* and the *re-oxidized* BiFeO₃ films reveals the formation of defect dipoles ($\text{Fe}^{2+}-\text{V}_\text{O}^{\bullet\bullet}$) as the main cause responsible for pinning. Re-oxidation treatment leads to the effective dissociation of these complexes to Fe^{2+} and $\text{V}_\text{O}^{\bullet\bullet}$, whose re-association is minimized by iron oxidation and oxygen vacancy compensation. Consequently, an enhanced domain mobility is obtained for the *re-oxidized* BiFeO₃ film with larger contribution to ferroelectric polarization. A remanent polarization of 67 $\mu\text{C cm}^{-2}$ is measured in this film that confirms its potential application in advanced devices and supports the tremendous expectation devoted to this multiferroic compound during the last years. The possible generation of new defect dipoles upon continued electric cycling or with time, which would affect the reliability of these *re-oxidized* BiFeO₃ films, is an area of future investigation.

This work was financed by Spanish Project No. MAT2010-15365. I.B. acknowledges the financial support of the Juan de la Cierva Spanish program. C.G.-L. acknowledges the financial support of the JAE-Tec (CSIC) Spanish program.

¹G. Catalán and J. F. Scott, *Adv. Mater.* **21**, 2463 (2009).

²J. B. Neaton, C. Ederer, U. V. Waghmare, N. A. Spaldin, and K. M. Rabel, *Phys. Rev. B* **71**, 014113 (2005).

³J. Wang, J. B. Neaton, H. Zheng, V. Nagarajan, S. B. Ogale, B. Liu, D. Viehland, V. Vaithyanathan, D. G. Schlom, U. V. Waghmare, N. A.

Spaldin, K. M. Rabe, M. Wuttig, and R. Ramesh, *Science* **299**, 1719 (2003).

⁴D. Lebeugle, D. Colson, A. Forget, M. Viret, P. Bonville, J. F. Marucco, and S. Fusil, *Phys. Rev. B* **76**, 024116 (2007); D. Lebeugle, D. Colson, A. Forget, and M. Viret, *Appl. Phys. Lett.* **91**, 022907 (2007).

⁵J. R. Teague, R. Gerson, and W. J. James, *Solid State Commun.* **8**, 1073 (1970).

⁶J. Dho, X. Qi, H. Kim, J. L. MacManus-Driscoll, and M. G. Blamire, *Adv. Mater.* **18**, 1445 (2006); S. M. Selbach, M.-A. Einarsrud, and T. Grande, *Chem. Mater.* **21**, 169 (2009).

⁷S.-H. Baek, C. M. Folkman, J.-W. Park, S. Lee, C.-W. Bark, T. Tybell, and C.-B. Eom, *Adv. Mater.* **23**, 1621 (2011).

⁸J. W. Park, S. H. Baek, P. Wu, B. Winchester, C. T. Nelson, X. Q. Pan, L. Q. Chen, T. Tybell, and C. B. Eom, *Appl. Phys. Lett.* **97**, 212904 (2010).

⁹F. Zavaliche, S. Y. Yang, T. Zhao, Y. H. Chu, M. P. Cruz, C. B. Eom, and R. Ramesh, *Phase Transition* **79**, 991 (2006); B. J. Rodriguez, Y. H. Chu, R. Ramesh, and S. V. Kalinin, *Appl. Phys. Lett.* **93**, 142901 (2008).

¹⁰C. Gutiérrez-Lázaro, I. Bretos, R. Jiménez, J. Ricote, H. El Hosiny, D. Pérez-Mezcua, R. J. Jiménez-Rioboó, M. García-Hernández, and M. L. Calzada, *J. Am. Ceram. Soc.* **96**, 3061 (2013).

¹¹G. L. Yuan, Y. Yang, and S. W. Or, *Appl. Phys. Lett.* **91**, 122907 (2007).

¹²T. Rojac, M. Kosec, B. Budic, N. Setter, and D. Damjanovic, *J. Appl. Phys.* **108**, 074107 (2010).

¹³W. L. Warren, D. Dimos, G. E. Pike, K. Vanheusden, and R. Ramesh, *Appl. Phys. Lett.* **67**, 1689 (1995).

¹⁴K. Yin, M. Li, Y. Liu, C. He, F. Zhuge, B. Chen, W. Lu, X. Pan, and R.-W. Li, *Appl. Phys. Lett.* **97**, 042101 (2010).

¹⁵H. Yang, Y. Q. Wang, H. Wang, and Q. X. Jia, *Appl. Phys. Lett.* **96**, 012909 (2010).

¹⁶E. Siegel and K. A. Müller, *Phys. Rev. B* **19**, 109 (1979).

¹⁷Y. Wang, Q.-H. Jiang, H.-C. He, and C.-W. Nan, *Appl. Phys. Lett.* **88**, 142503 (2006).

¹⁸R. Jiménez, C. Alemany, M. L. Calzada, A. González, J. Ricote, and J. Mendiola, *Appl. Phys. A: Mater. Sci. Process.* **75**, 607 (2002).

¹⁹S. L. Miller, R. D. Nasby, J. R. Schwank, M. S. Rodgers, and P. V. Dresendorfer, *J. Appl. Phys.* **68**, 6463 (1990).

²⁰J. Wang, H. Zheng, Z. Ma, S. Prasertchoung, M. Wuttig, R. Droopad, J. Yu, K. Eisenbeiser, and R. Ramesh, *Appl. Phys. Lett.* **85**, 2574 (2004); J. Wu and J. Wang, *J. Appl. Phys.* **106**, 104111 (2009).